

Series array of incommensurate superconducting quantum interference devices from $\text{YBa}_2\text{Cu}_3\text{O}_{7-\delta}$ ion damage Josephson junctions

Shane A. Cybart,^{a)} S. M. Wu, S. M. Anton, I. Siddiqi, John Clarke, and R. C. Dynes

Department of Physics, University of California, Berkeley, California 94720-7300, USA

and Materials Sciences Division, Lawrence Berkeley National Laboratory, Berkeley, California 94720, USA

(Received 1 October 2008; accepted 15 October 2008; published online 3 November 2008)

We have fabricated a series array of 280 superconducting quantum interference devices (SQUIDs) using $\text{YBa}_2\text{Cu}_3\text{O}_{7-\delta}$ thin film ion damage Josephson junctions. The SQUID loop areas were tapered exponentially so that the response of the current-biased array to magnetic field is a single voltage spike at zero field. We fitted the current-voltage characteristics of the array to a model in which we summed the voltages across the SQUIDs assuming a resistively shunted junction model with a normal distribution of SQUID critical currents. At 75 K the standard deviation of these critical currents was 12%. © 2008 American Institute of Physics. [DOI: 10.1063/1.3013579]

There recently has been interest in studying arrays of superconducting quantum interference devices (SQUIDs) with incommensurate areas. The critical currents of SQUIDs in such an array oscillate with incommensurate periodicities as a function of applied magnetic field B . As a result, the critical current of the array attains a maximum value at zero magnetic field, but is nearly zero elsewhere. Consequently, for Josephson junctions with nonhysteretic current-voltage (I - V) characteristics, the current-biased array exhibits a single sharp minimum in voltage at zero field. This behavior was first demonstrated by Sohn *et al.*¹ using two-dimensional (2D) arrays of Nb– AlO_x –Nb Josephson junctions, and later Carelli *et al.*² showed that one could use a series array of incommensurate SQUIDs as an absolute vector magnetometer. More recently, arrays of incommensurate SQUIDs made from the high-transition temperature (T_c) superconductor $\text{YBa}_2\text{Cu}_3\text{O}_{7-\delta}$ (YBCO) have been fabricated with loops connected in series, parallel, and a series-parallel combination.^{3–5} Schultze *et al.*³ demonstrated large transfer coefficients $V_B \equiv |\partial V / \partial B|_I$ despite spreads in the parameters of the junctions, notably their critical currents and resistances. It has been suggested that it may be possible to use incommensurate SQUID arrays as radio frequency (rf) amplifiers.⁶

Previous incommensurate high- T_c SQUID arrays have been fabricated from bicrystal grain boundary Josephson junctions.^{3,7} Because the locations of these Josephson junctions are constrained to a single grain boundary, it is difficult to design high-frequency devices, for which it is desirable to incorporate the array into a transmission line, for example a microstrip or a coplanar waveguide. One way to overcome this constraint is to use high- T_c Josephson junctions with barriers formed by ion damage. Such junctions were first realized in 1990 by Tinchev⁸ and since have been studied by several groups.^{9–11} Single rf and dc SQUIDs have been fabricated from these junctions,^{12,13} and series arrays of tens of junctions have shown potential for voltage standard applications.^{14,15} In this letter we describe the fabrication and measurement of a SQUID array comprised of ion damage Josephson junctions.

A 200 nm thick YBCO thin film¹⁶ on sapphire with a

gold contact layer deposited *in situ* was patterned using photolithography and Ar^+ ion milling to fabricate a 50 Ω coplanar waveguide with 280 SQUID loops etched into the signal line [Fig. 1(a)]. We chose a coplanar waveguide configuration for efficient coupling of rf signals in future experiments. The width of the signal conductor containing the chain of SQUID loops was tapered linearly, resulting in areas that tapered exponentially from 1600 to 1 μm^2 . In the next step we constructed a trilayer mask for ion implantation. The wafers were coated with a 700 nm layer of hard-baked photoresist that served as the ion stopping layer. A 25 nm layer of Ge was evaporated onto the resist and served as an etch stop. We next spun on 100 nm of polymethylmethacrylate (PMMA) resist for electron-beam lithographic patterning. Using a customized 100 keV Leica VB6-HR, we wrote 30 nm lines in the PMMA over the locations intended for junctions. This pattern was transferred into the Ge layer with reactive ion etching (RIE) in a $\text{HBr}-\text{Cl}_2$ plasma. The pattern in the Ge was transferred to the resist using low temperature (-100°C), low pressure (5 mtorr) oxygen RIE. This process resulted in a high aspect ratio of the line width to the trench height (23:1) because the etch selectivity between Ge and resist in oxygen plasma is very large (>100). Following the etching, the wafers were implanted commercially with 200 keV Ne^+ at a dose of 1×10^{13} ions/ cm^2 . The T_c of the

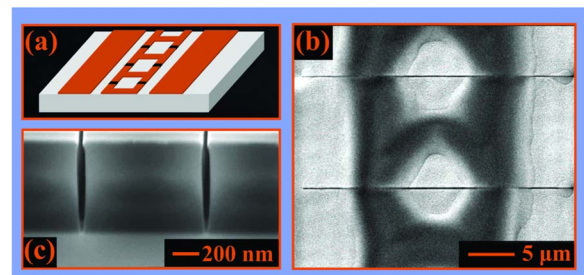


FIG. 1. (Color online) Device layout and fabrication. (a) Illustration of a segment of the coplanar wave guide containing a SQUID array showing the placement of the junctions. The SQUID loops are 5 μm wide. (b) Top view SEM image of the implantation mask above the YBCO device. The edges appear poorly defined because of the protective layer of resist draped over the YBCO. The dark horizontal lines are the nanopatterned slits used to form the junctions. (c) Cross-section view of a high aspect ratio implantation mask.

^{a)}Electronic mail: scybart@berkeley.edu.

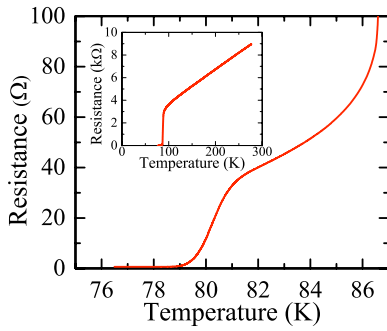


FIG. 2. (Color online) Resistance vs temperature for an array of 280 YBCO SQUIDs measured at 10 μ A. Inset shows the data over a larger temperature range.

YBCO not protected by the hard mask was lowered by disorder, forming S' regions of the planar inline $SS'S$ junctions, where S' and S denote superconductors with and without damage, respectively. Figure 1(a) shows a drawing of three (of the 280) SQUID loops and the placement of the junctions. The two strips of conductor on either side of the SQUID chain serve as the ground plane for a coplanar waveguide microwave transmission line. A top view scanning electron microscope (SEM) image of the trilayer mask above two loops is shown in Fig. 1(b). The cuts in the mask were measured to be 30 nm wide. A test sample of silicon with the same trilayer mask was etched simultaneously with the YBCO wafer and cleaved for cross-sectional viewing. This process enabled us to ensure that the mask was etched completely and that there was minimal undercutting [Fig. 1(c)].

Completed devices were attached to a printed circuit board (PCB) equipped with π -filters and a silicon diode thermometer. The board was surrounded with a $\text{Bi}_2\text{Sr}_2\text{Ca}_2\text{Cu}_3\text{O}_{10}$ superconducting shield mounted inside a vacuum probe equipped with an outer Cryoperm shield. The probe was cooled in a liquid nitrogen bath that could be pumped to temperatures as low as 65 K. We measured the resistance of the device as a function of decreasing temperature using a lock-in amplifier and a 22 Hz, 10 μ A amplitude current. The device exhibited two distinct superconducting transitions. The temperatures at the transition midpoints were 87.5 ± 0.2 K for the bulk YBCO [Fig. 2 (inset)] and 80.3 ± 0.2 K for the ion damaged weak links (Fig. 2). Thus, the ion damage reduced the T_c by about 7 K. The width of the weak-link superconducting transition was comparable to that of the bulk material, indicating that the homogeneity of T_c in the weak-link region was as uniform as that of the bulk material, and that the ion damage was uniform.

We measured I - V characteristics for the array, shown in Fig. 3 for $B=0$ at four temperatures. Assuming the resistively shunted junction model^{17,18} and that all SQUIDs have resistance R_s and a random normal distribution of critical currents I_{sk} , we fitted the data with $V = R_s \sum_{k=1}^{280} (I^2 - I_{sk}^2)^{1/2} (I > I_{sk})$. Here, $I_{sk} = \bar{I}_s(1 + \delta_k)$, where \bar{I}_s is the mean SQUID critical current at $B=0$ and δ_k is the fractional variation in the critical currents. Noise rounding was not included because it has been shown to be small in comparison to rounding from nonuniform critical currents for these values of I_s .¹⁹ By fitting the I - V characteristics at various temperatures, we determined that the standard deviation of the parameter δ_k ranges from 0.50 at the highest temperatures to a minimum of 0.12 at 75 K. These fits also yield \bar{I}_s and R_s as functions of temperature,

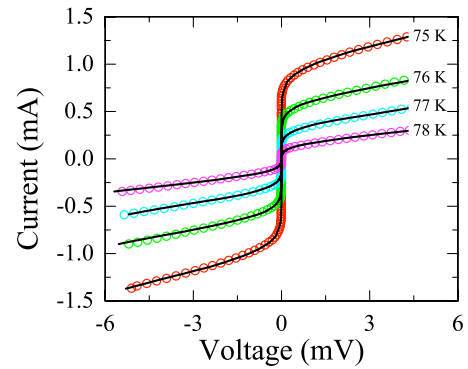


FIG. 3. (Color online) Current-voltage characteristics measured at four temperatures with $B=0$. Solid lines are fits to the data (circles).

shown in Fig. 4. The resistance increases rapidly with temperature and the linear fit shows that \bar{I}_s scales as $(1 - T/T_c)^2$, consistent with data from other ion damage junctions.²⁰ The value of T_c was determined to be 80.1 ± 0.2 K, in good agreement with the value obtained from Fig. 2. The $\bar{I}_s R_s$ product versus T shows a peak near 75 K.

To characterize the response of the device to magnetic field, we biased the array with a static current I_b and measured the voltage at seven temperatures as we swept the magnetic field. Figure 5(a) shows the data for $I_b = 1.5I_a$, where I_a is the critical current of the array. The data show a broad dip with a maximum amplitude at 75 K, the temperature at which $\bar{I}_s R_s$ is a maximum. An additional sharper spike with an amplitude of 50 μ V [Fig. 5(a) inset] is observed at higher temperatures. We have reproduced these two regimes in simulations.²¹ The results of V - B measurements for different bias currents at 75 K are shown in Fig. 5(b). For $I_b = 1.0I_a$, the voltage response is flat at zero field, reflecting the fact that the array is biased at the minimum I_{sk} . At 75 K with $I_b = 1.5I_a$, the broad dip amplitude is 3.3 mV with a 47 μ T full width at half maximum (FWHM) determined from a Lorentzian fit of the data. As the bias is increased above $1.5I_a$, the dip amplitude decreases and the FWHM increases [Fig. 5(c)]. The maximum value of V_B was determined to be 105 V/T for the broad dip and 45 V/T for the sharp spike. These values are about an order of magnitude lower than previous results³ but are consistent with simulations²¹ for parameters chosen for our device.

The authors thank Larry Larson for assisting with device design, Bruce Harteneck for helping with the device fabrication, Y. H. Chen for PCB layout, and J. J. Lee for help

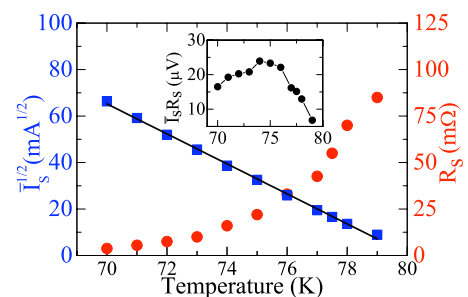


FIG. 4. (Color online) $\bar{I}_s^{1/2}$ (squares) and R_s (circles) vs temperature determined from fitting the I - V characteristics. The inset shows the $\bar{I}_s R_s$ product vs temperature.

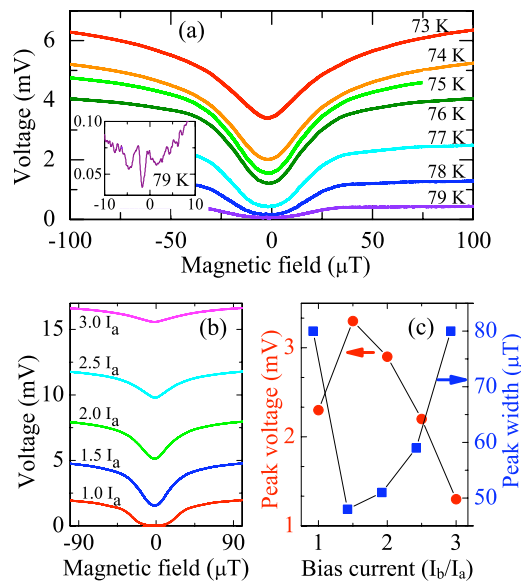


FIG. 5. (Color online) Voltage vs magnetic field characteristics. (a) V vs B for $I_b = 1.5 I_a$ measured at seven temperatures. Inset shows expanded view. (b) V vs B at 75 K for five values of I_b . (c) Peak height in mV (circles) and peak width in μT (squares) at 75 K vs bias current normalized to I_a .

assembling the measurement system. This work was supported by AFOSR Grant No. FA9550-05-1-0436, and ONR Grant No. N00014-07-1-0774 (Siddiqi). The EBL and RIE at the Molecular Foundry were supported by the Office of Science and Office of Basic Energy Sciences of the U.S. Department of Energy under Contract No. DE-AC02-05CH11231.

- ¹L. L. Sohn, M. T. Tuominen, M. S. Rzchowski, J. U. Free, and M. Tinkham, *Phys. Rev. B* **47**, 975 (1993).
- ²P. Carelli, M. G. Castellano, K. Flacco, R. Leoni, and G. Torrioli, *Europhys. Lett.* **39**, 569 (1997).
- ³V. Schultze, R. IJsselsteijn, H.-G. Meyer, J. Oppenlander, C. Häussler, and N. Schopohl, *IEEE Trans. Appl. Supercond.* **13**, 775 (2003).
- ⁴A. V. Shadrin, K. Y. Constantinian, and G. A. Ovsyannikov, *Tech. Phys. Lett.* **33**, 192 (2007).
- ⁵O. Snigirev, M. Chukharkin, A. Kalabukhov, M. Tarasov, A. Deleniv, O. Mukhanov, and D. Winkler, *IEEE Trans. Appl. Supercond.* **17**, 718 (2007).
- ⁶V. Kornev, I. Soloviev, N. Klenov, and O. Mukhanov, *IEEE Trans. Appl. Supercond.* **17**, 569 (2007).
- ⁷P. Caputo, J. Oppenländer, C. Häussler, J. Tömes, A. Friesch, T. Träuble, and N. Schopohl, *Appl. Phys. Lett.* **85**, 1389 (2004).
- ⁸S. S. Tinchev, *Supercond. Sci. Technol.* **3**, 500503 (1990).
- ⁹R. Barth, A. H. Hamidi, B. Hadam, J. Hollkott, D. Dunkmann, J. Auge, and H. Kurz, *Microelectron. Eng.* **30**, 407 (1996).
- ¹⁰A. S. Katz, A. G. Sun, S. I. Woods, and R. C. Dynes, *Appl. Phys. Lett.* **72**, 2032 (1998).
- ¹¹N. Peng, D. J. Kang, C. Jeynes, R. P. Webb, D. F. Moore, M. G. Blamire, and I. Chakarov, *IEEE Trans. Appl. Supercond.* **13**, 889 (2003).
- ¹²S. S. Tinchev, *IEEE Trans. Appl. Supercond.* **3**, 28 (1993).
- ¹³N. Bergeal, J. Lesueur, G. Faini, M. Aprili, and J. P. Contour, *Appl. Phys. Lett.* **89**, 112515 (2006).
- ¹⁴K. Chen, S. A. Cybart, and R. C. Dynes, *Appl. Phys. Lett.* **85**, 2863 (2004).
- ¹⁵S. A. Cybart, K. Chen, and R. C. Dynes, *IEEE Trans. Appl. Supercond.* **15**, 241 (2005).
- ¹⁶Purchased from Theva Dünnschichttechnik GmbH, Rote-Kreuz-Str. 8, D-85737, Ismaning, Germany.
- ¹⁷D. E. McCumber, *J. Appl. Phys.* **39**, 3113 (1968).
- ¹⁸W. C. Stewart, *Appl. Phys. Lett.* **12**, 277 (1968).
- ¹⁹S. A. Cybart, "Planar Josephson junctions and Arrays by electron beam lithography and ion damage," Ph.D. thesis, University of California, 2005.
- ²⁰A. S. Katz, S. I. Woods, and R. C. Dynes, *J. Appl. Phys.* **87**, 2978 (2000).
- ²¹S. M. Wu, S. A. Cybart, S. M. Anton, I. Siddiqi, J. Clarke, and R. C. Dynes (unpublished).